5-2003

Design of a rocker arm for a high performance engine

Stephen Edward Stewart

To the Graduate Council:

I am submitting herewith a thesis written by Stephen Edward Stewart entitled "Design of a rocker arm for a high performance engine." I have examined the final electronic copy of this thesis for form and content and recommend that it be accepted in partial fulfillment of the requirements for the degree of Master of Science, with a major in Mechanical Engineering.

Frank Speckhart, Major Professor

We have read this thesis and recommend its acceptance:

Accepted for the Council:
Dixie L. Thompson

Vice Provost and Dean of the Graduate School

(Original signatures are on file with official student records.)

To the Graduate Council:

I am submitting herewith a thesis written by Stephen Edward Stewart entitled "Design of a Rocker Arm for a High Performance Engine." I have examined the final paper copy of this thesis for form and content and recommend that it be accepted in partial fulfillment of the requirements for the degree of Master of Science, with a major in Mechanical Engineering.

Frank Speckhart

Dr. Frank Speckhart, Major Professor

We have read this thesis
and recommend its acceptance:

John D. Landes

Acceptance for the Council:

Vice Provost and Dean of Graduate Studies

Design of a Rocker Arm for a High Performance Engine

A Thesis
Presented for the
Master of Science Degree
The University of Tennessee, Knoxville

Stephen Edward Stewart
May 2003

ABSTRACT

The purpose was to improve an existing design of a rocker arm for a high performance engine. The design used as the baseline design was a solid aluminum Jesel rocker arm. This improvement was to be accomplished through two designs, one having lower rotational inertia with the same stiffness and another having the same rotational inertia and higher stiffness.

The analysis and design were accomplished by using a numerical integration program, experimentation, and finite element analysis. The numerical integration program was written to model the rocker arm designs. This allowed design changes to be efficiently evaluated. The accuracy of the numerical integration was verified by comparing results for the Jesel rocker arm with data collected through experimentation. A finite element model was made to further analyze the rocker arm designs.

Significant improvements to the baseline rocker arm were expected. The actual results obtained were marginal improvements on the baseline design. The higher than expected shear deflection was a limiting factor in making the improvements.

TABLE OF CONTENTS

LIST OF TABLES

LIST OF FIGURES

LIST OF SYMBOLS

b = Width

d = Distance Between Parallel Axes

E = Modulus of Elasticity

F = Force

h = Height

I = Moment of Inertia

J = Rotational Inertia

J_{cg} = Rotational Inertia Center of Gravity

k = Stiffness

k_{sf} = Shape Factor

M = Moment

m = Mass

q = Web Thickness

t = Width

V = Volume

y = Deflection

y_s = Shear Deflection

y_t = Total Deflection

ρ = Density

υ = Poisson's Ratio

INTRODUCTION

The purpose of this thesis was to improve an existing design of a rocker arm for a high performance engine. The current design, which will be used as the baseline design, is a rocker arm manufactured by the company Jesel. It consists of solid aluminum and is made for a pushrod engine. The Jesel rocker arm is considered to be the racing industry standard. The rocker arm has a ratio of 1.8 to 1 for the valve side length to the pushrod side length. The major dimensions of the baseline rocker arm can be seen in figure 1. Modifications to the baseline rocker arm will result in improvements to the rotational inertia and stiffness in two separate designs. The rotational inertia, J, and stiffness, k, are defined as

$J = \int r^2 dm$ (Hibbeler, 1995)

$k = \dfrac{F}{y_t}$ (Thomson and Dahleh, 1998).

The design specifications for the two designs are the following:

- Reduce the rotational inertia while maintaining the same stiffness as the baseline
- Increase the stiffness while maintaining the same rotational inertia as the baseline

The height, width, and cross section of the baseline were changed to find a design that best met the design specifications. Due to the relatively low rotational inertia and high stiffness of the pushrod side of the rocker arm, analysis for improving the rocker arm was restricted to the valve side. The design parameters identified through this analysis could also be applied to the pushrod side. Initially, both I-beam and H-beam cross sections were considered. The I-beam cross section was chosen because calculations showed that

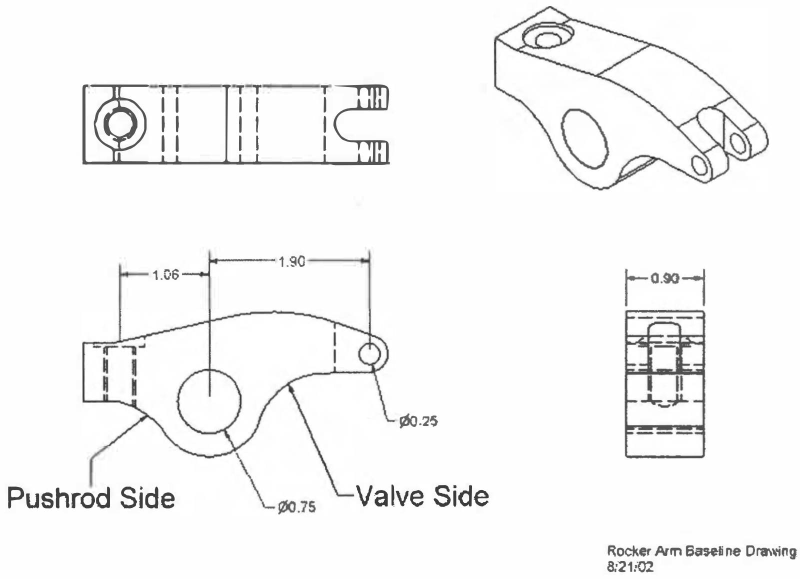

Figure 1. Baseline Rocker Arm Major Dimensions

for the same height, width, and web thickness the I-beam had smaller rotational inertia and smaller deflection. The sample calculations can be seen in figure A-1. Numerical integration, three-dimensional drawings, experimentation, and finite element analysis were the tools used in designing the new rocker arms.

1 APPROACH

1.1 Three-Dimensional Drawing

A three-dimensional drawing was made of the baseline rocker arm. The necessary dimensions were gathered using calipers, rulers, and a compass to produce a drawing. AutoDesk Inventor was chosen as the drawing package to produce a three-dimensional model. This was a user-friendly program in all aspects of drawing, extruding, cutting, and modifying. One advantage of Inventor was the ability to take multiple parts and combine them into a single assembly. Inventor also made three-view drawings quickly with dimensions automatically placed on the drawing. This part of the program allowed the user to choose which view would be the primary view and then project the other views. Inventor displayed the physical properties of the part such as the location of the center of gravity, mass, mass moment of inertia, surface area, and volume.

1.2 Computer Model

Once the drawing of the baseline rocker arm was complete, fourteen points from the top profile and fourteen points from the bottom profile were recorded. Figure 2 shows the points chosen for the top and bottom profiles. A computer program was written to linearly interpolate between points to increase the number of data points. The points were plotted using Excel. The curves for both the top and bottom profiles were sixth degree polynomials. Figure 3 shows the curve fit through the data points.

There are several equations that were used in analyzing the baseline and prospective rocker arms. The equation used to compute the rotational inertia is

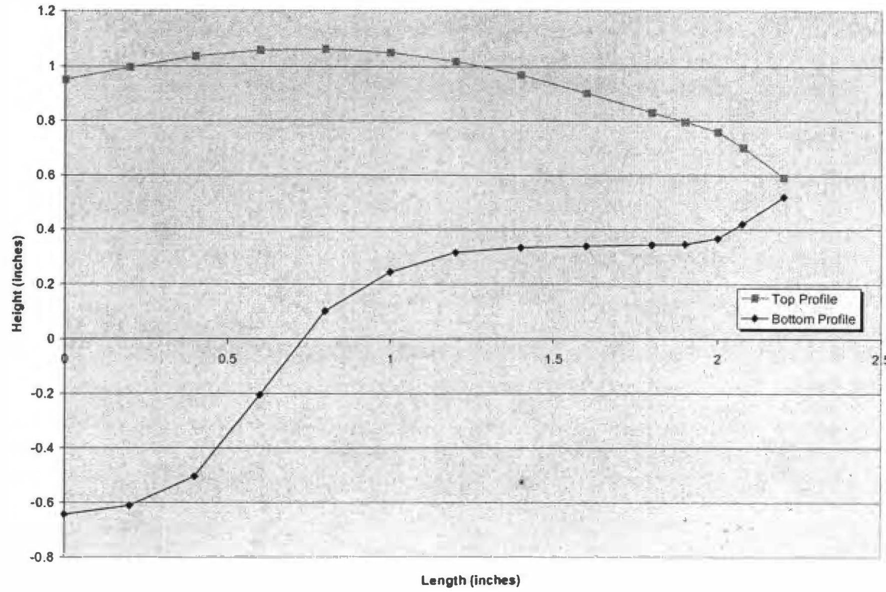

Figure 2. Points chosen for Top and Bottom Profile for Baseline Rocker Arm

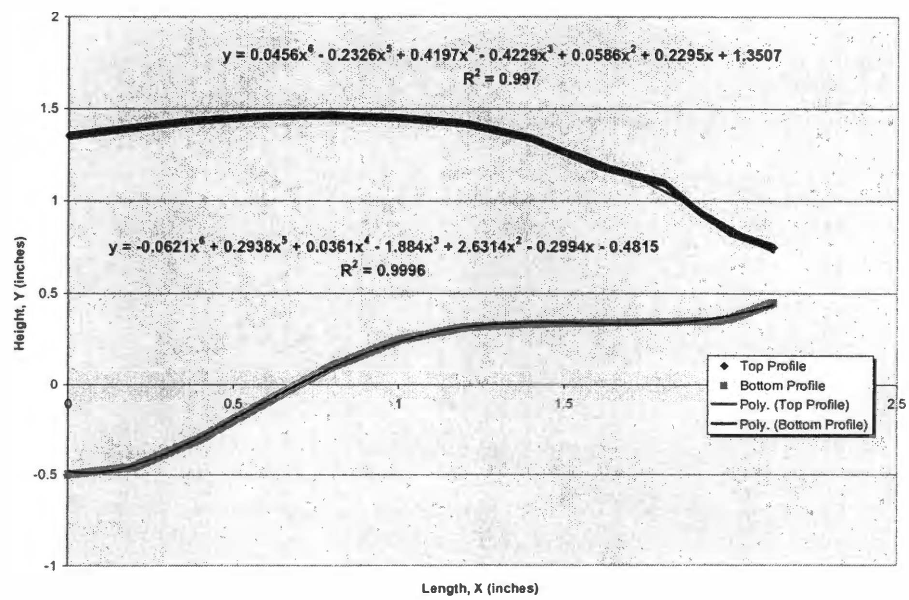

Figure 3. Curve fit through Top and Bottom Profile

$J = \int r^2 dm = \int r^2 \rho dV$ (Hibbeler, 1995)

The parallel-axis theorem allows the transfer of rotational inertia from the center of gravity to any parallel axis

$J = J_{cg} + md^2$ (Hibbeler, 1995)

The equation used to determine the deflection due to bending was

$\frac{d^2 y}{dx^2} = \frac{M(x)}{EI(x)}$ (Hibbeler, 1994)

where

$I = \frac{bh^3}{12}$ (Rectangular Cross Section) (Hibbeler, 1994)

$I = \frac{bh^3}{12} - \frac{2(b-q)(h-2q)^3}{12}$ (I Cross Section)

The dimensions for the I cross section are defined in figure 4.

Shear deflection was initially left out of the numerical integration program and was added once the magnitude of the shear deflection was realized. The shear deflection turned out to be the same magnitude as the bending deflection. The shear deflection equation used was

$y_s = \int \frac{k_{sf} F}{AG} dx$ (Cook and Young, 1999)

The shape factor k_{sf} is dependent on the cross section analyzed. The shape factor for a solid rectangle is 1.2 (Cook and Young, 1999). An I beam shape factor was calculated from

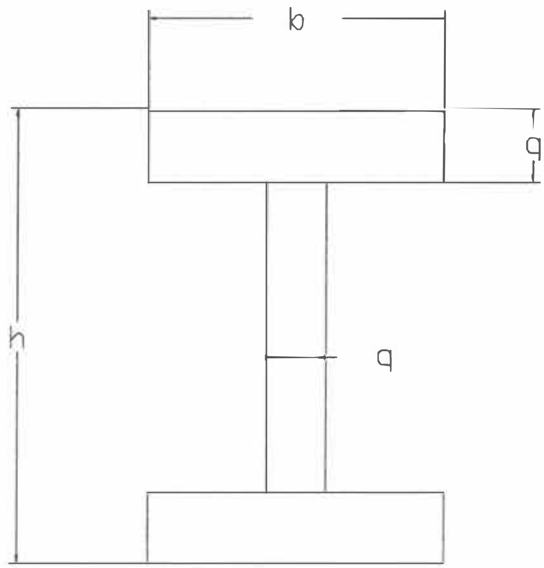

Figure 4. I Cross Section

$$k_{sf} = \frac{(12+72m+150m^2+90m^3)+\upsilon(11+55m+135m^2+90m^3)}{10(1+\upsilon)(1+3m)^2} +$$

$$\frac{30n^2(m+m^2)+5\upsilon n^2(8m+9m^2)}{10(1+\upsilon)(1+3m)^2} \text{ (Cowper, 1966)}$$

where

$$m = \frac{2tq}{hq}$$

$$n = b/h$$

The shape factor was calculated for the new rocker arms and it ranged from 2 – 3.3 depending on the distance from the pivot. The actual shape factor used in the computer programs was 2.35. This shape factor was determined by iteration to match the finite element result. The total deflection of the rocker arms was calculated by

$$y_t = y + y_s$$

The stiffness was calculated by

$$k = \frac{F}{y_t} \text{ (Thomson and Dahleh, 1998)}$$

These equations were all used in the numerical integration program for the baseline and new designs. The programs were set up to integrate distinct sections of the rocker arm such as the hole, middle section and end cutout. The baseline program and the I-beam program can be seen in Figures A-2 and A-3 respectively.

The top profile was changed by adding the y values of a linear function to the y values of the top profile to see if a better top profile existed. Numerical Integration was used to add the linear functions to the top profile. Figure 5 shows the linear functions

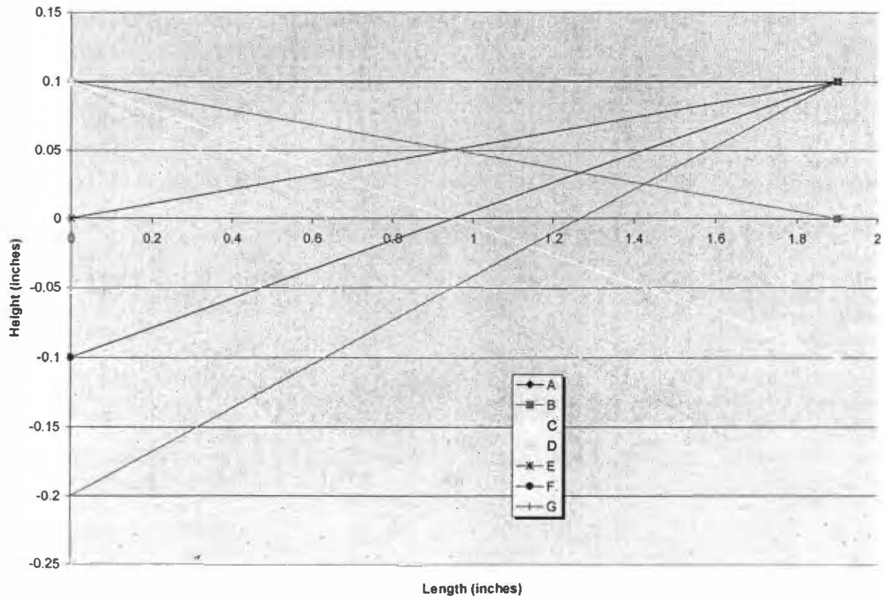

Figure 5. Linear Functions for Changing Top Profile

chosen to change the top profile. Figure 6 shows the results of adding the linear functions to the top profile. Table 1 shows the results of changing the top profile. The results show that the best curve is adding a horizontal line, which simply raises the top profile.

The low inertia rocker arm with the I cross section and the raised top profile was drawn and analyzed using Inventor. The rotational inertia of this rocker arm was higher than the rotational inertia of the baseline rocker arm. Therefore, a new top curve was needed to reduce the rotational inertia. The curve was changed to reduce the mass at the end of the rocker arm. The Inventor drawing of the low inertia rocker arm was used to cut away mass at the end of the valve side. Figure 7 shows the comparison of Inventor drawings of the low inertia design with the raised baseline top profile and the new top profile. The new points were plotted in Excel and can be seen in figure 3. The results of the numerical integration program are based on this new top profile curve. The computer program was used to change the width, height, and web thickness to determine the effects on stiffness and rotational inertia. These changes could be accomplished much faster than drawing the part and analyzing it in the finite element program.

1.3 Experiment of Baseline Rocker Arm

An experiment was designed to measure the actual deflections of the valve side and pushrod side of the baseline rocker arm. An Instron machine was chosen to produce the needed compressive force. The Instron machine used was screw driven with a moving cross head with a maximum force of 20,000 lbs. Examination of the Instron machine

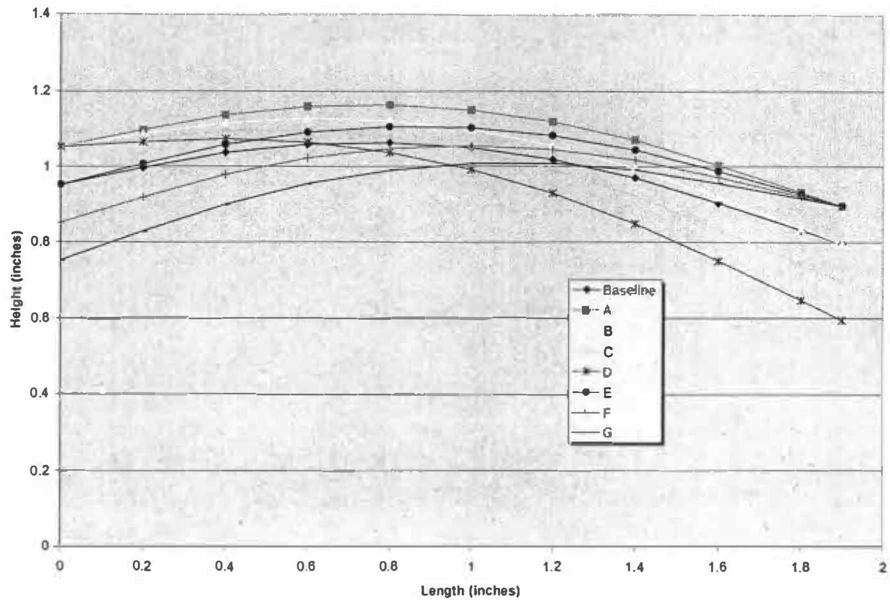

Figure 6. The Results of Adding Linear Functions to the Baseline Top Profile

Table 1. Results of Changing the Top Profile

X	A	B	C	D	E	F	G
0	0.1	0.1	0.1	0.1	0	-0.1	-0.2
1.9	0.1	0	-0.1	-0.2	0.1	0.1	0.1
J (in*lb*sec^2)	0.987	0.935	0.886	0.839	0.947	0.91	0.876
y (in)	0.00090	0.00102	0.00118	0.00141	0.00102	0.00116	0.00133
J/k (in^3*sec^2)	8.9E-07	9.5E-07	1.0E-06	1.2E-06	9.7E-07	1.1E-06	1.2E-06
stress max (psi)	10877	11864	13034	15103	11758	12776	13963
x@stressmax (in)	1.00	1.00	1.076	1.20	1.00	1.00	1.00
Thk (in)	0.9	0.9	0.9	0.9	0.9	0.9	0.9
web thk (in)	0.125	0.125	0.125	0.125	0.125	0.125	0.125

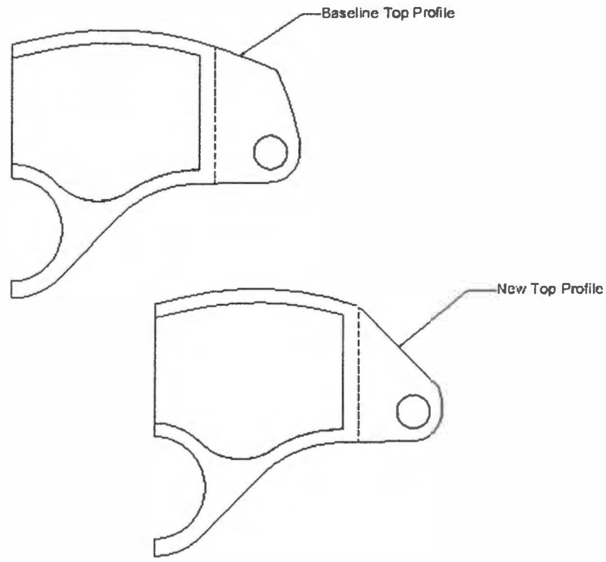

Figure 7. Comparison of Baseline Top vs New Top Profile

revealed that a test stand needed to be designed and manufactured. The test stand was needed to hold the rocker arm higher than the automatic stops of the cross head and had to be tall enough to accommodate the dial indicators needed to measure the deflections. Figure A-4 shows the test stand and its dimensions. The test stand cutout for the shaft had to be shifted back from the center to accommodate the dial indicator for the pushrod side. The other necessary part of the test stand was the top plate which can be seen in Figure A-5. The flat portion of the top plate was designed to contact the cross head. The top plate also contained the valve side and pushrod pins to transfer the force to the valve side and pushrod side of the rocker arm. The dimensions of the pushrod and valve side pins were determined to minimize rotation of the rocker arm. These dimensions of the pushrod and valve side pins can be seen in Figure A-6. Figure A-7 shows an assembly drawing of the test stand. This assembly drawing ensured that all of the components of the test stand would fit together properly. Before the experiment was begun, the Instron machine was calibrated and the test stand assembled. The calibration process included ensuring that the full scale output was equal to 100% of the scale chosen and that output was initially at zero. The test stand was placed into position underneath the cross head. The 0.0001 inch resolution dial indicators were placed on the valve side and pushrod side using magnetized stands. Figure 8 shows a picture of the experimental setup. The applied force began at zero pounds and went to a maximum of 3000 pounds. Several tests were performed to ensure repeatability in the results. Figure 9 shows the test results. The deflections measured in the tests were higher than anticipated. It was determined that the shaft the rocker arm pivots around was deflecting under the applied load. To

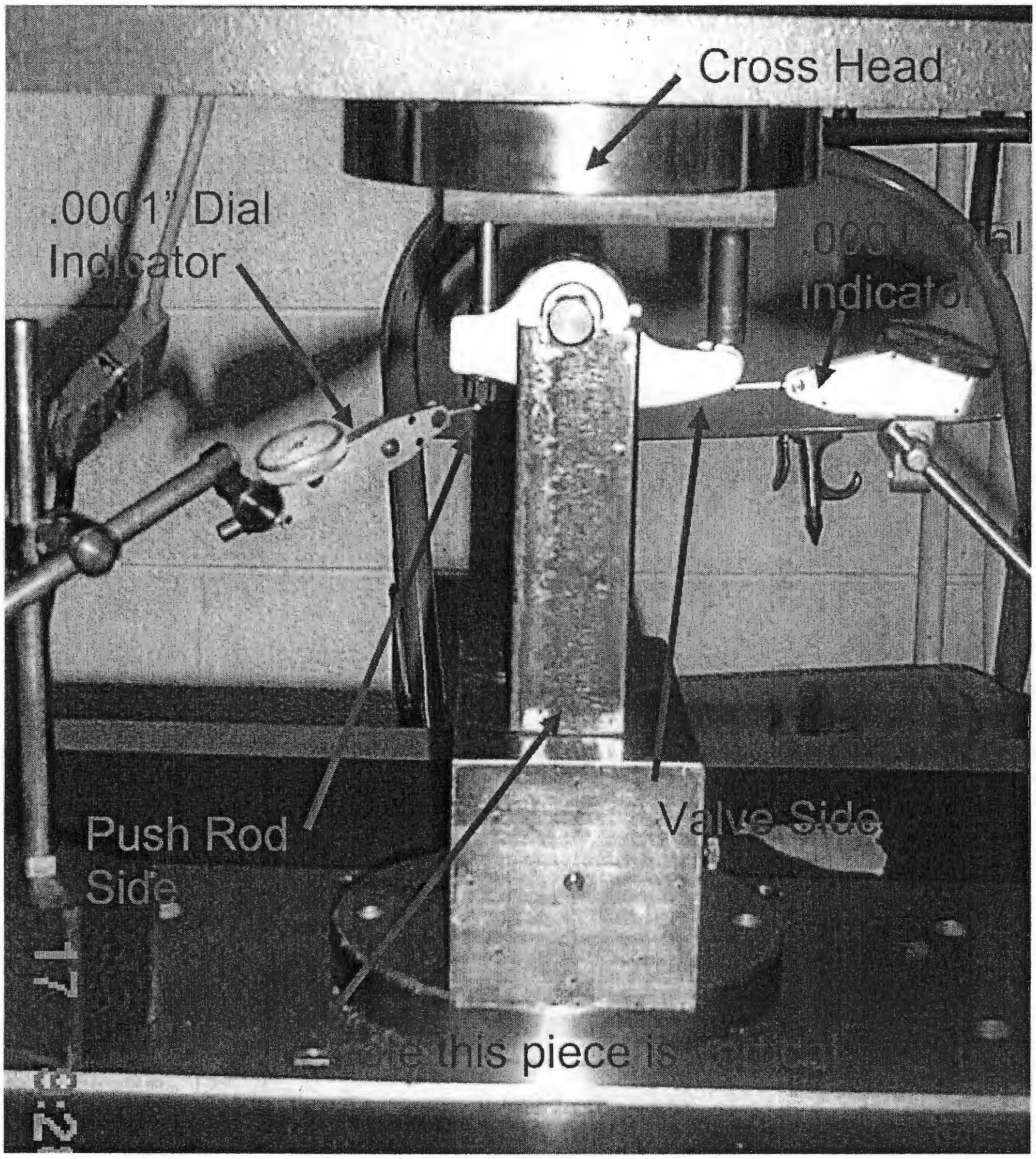

Figure 8. Picture of Experimental Setup

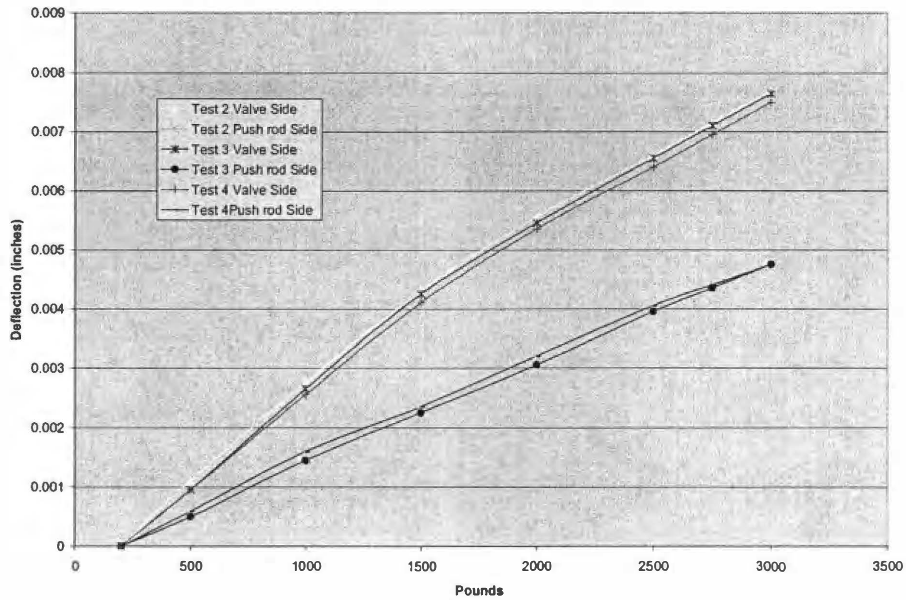

Figure 9. Baseline Rocker Arm Experiment Test Results

measure the deflection of the shaft, a dial indicator was placed on top of the bottom profile as shown in Figure 10. Figure 11 shows the results of this measurement. Figure 12 shows the adjusted results of using the center deflection. The adjusted test results were calculated by subtracting the center deflections from the test results. The adjusted valve side deflection was determined to be 0.0047 inch, and the adjusted pushrod side deflection was determined to be 0.0018 inch.

1.4 Finite Element Analysis

Two finite element analysis packages were evaluated to select which package would be used for the analysis. Initially, Cosmos Design Star was evaluated. Cosmos, a stand-alone program, allowed the importing of three-dimensional models from Inventor. The rocker arm was modeled two ways. The first way the rocker arm was modeled was the whole rocker arm supported by a shaft. The other was the valve side and pushrod side halves being individually supported at the ends near the pivot. This support modeled the separate halves as a cantilever beam. Comparing the results of both runs revealed that the deflections were the same whether modeled by the whole rocker arm or the cantilever beam. After the comparison was completed all subsequent finite element runs were completed by modeling the rocker arm as a cantilever beam. Different loads were applied to the valve side and the deflections that resulted were not linear. Cosmos showed that for a linear increase in force, the resulting deflection was not linear. The test results and numerical integration showed a linear relationship between force and deflection. Since stresses were below yield, this indicated a serious problem with

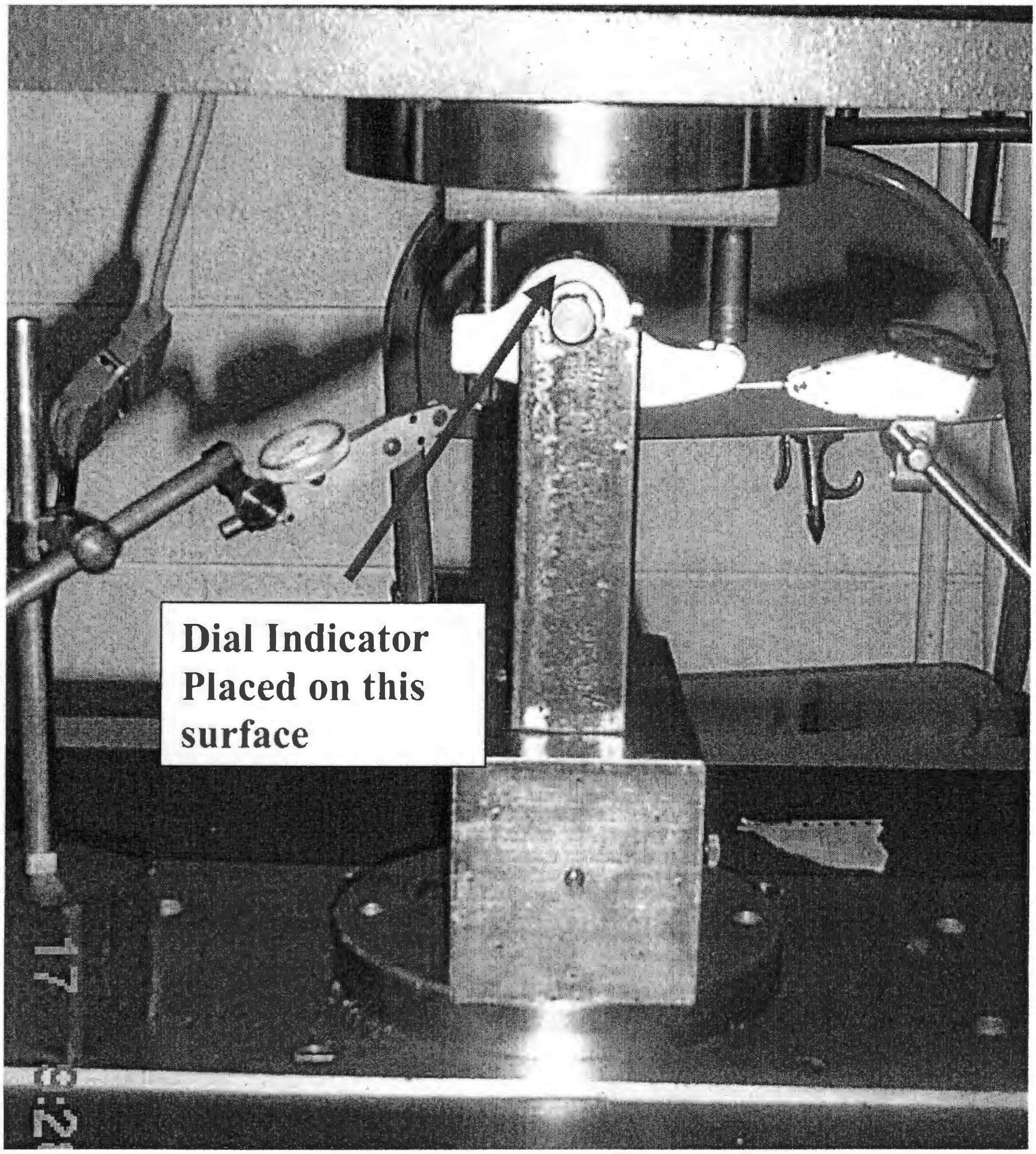

Figure 10. Picture of Experiment with Additional Dial Indicator Placement

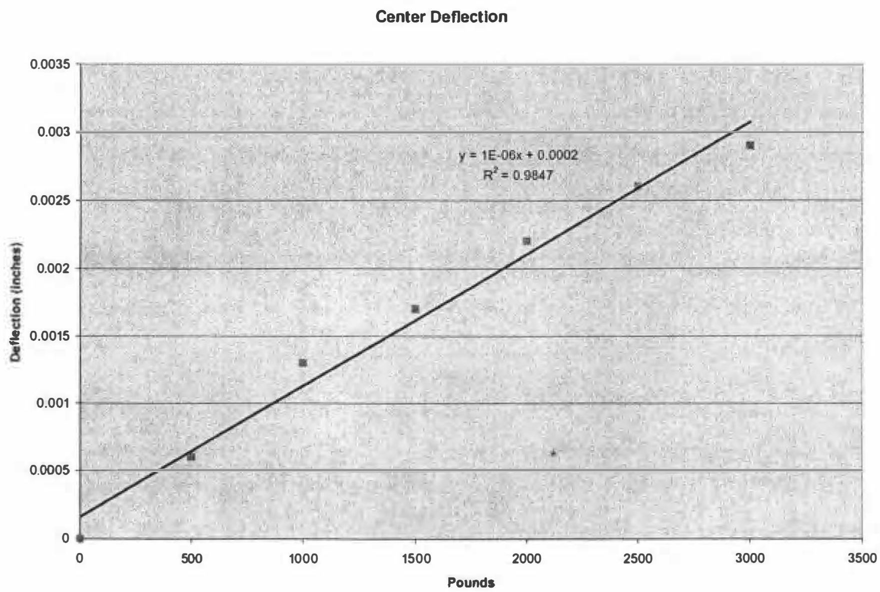

Figure 11. Baseline Rocker Arm Center Deflection Results

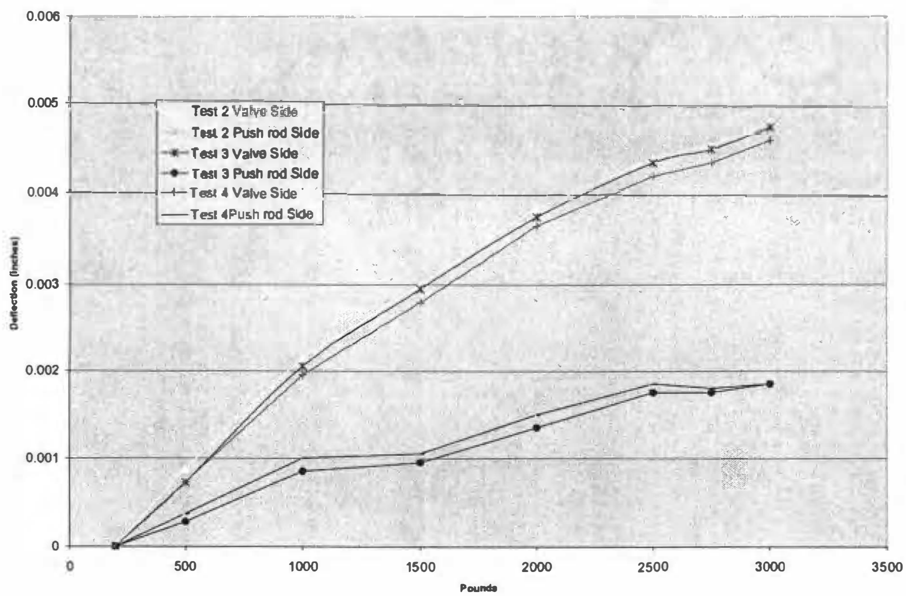

Figure 12. Baseline Rocker Arm Adjusted Center Deflection Results

Cosmos. Since Cosmos was not consistent with experimentation and numerical integration a new finite element package was used. Ansys Design Space was tried and ultimately chosen to analyze the baseline rocker arm and the two new designs. There were several steps to be completed before obtaining the solutions from Ansys. The first step was to insert the three-dimensional model of the part or assembly. The next step was to assign a specific material to the part or assign different materials to each part in the assembly. The next step was to insert the load. The load chosen for the rocker arm was force applied to the pin on the valve side. After the magnitude and direction of the force were entered, the supports were inserted. Two of the supports were used in the analysis. For the modeling of the entire rocker arm the pivot was supported using a cylindrical support and the sides were supported using frictionless supports. The cylindrical support was chosen to model the pivot. The frictionless supports were chosen to support any rotations caused by any unbalance of forces. Figure 13 shows the cylindrical support and Figure 14 shows the frictionless supports. The other model used fixed supports to model the pushrod half and the valve side half as cantilever beams. The deflection results of the two models matched. The two separate models were compared using the results of the total deflection. The total deflection of both sides of the arm using the cantilever analysis matched the deflection of the frictionless support. All other subsequent runs utilized the cantilever supports for the valve side. The final step was to solve for stress, total deformation, and directional deformation. The probe in Ansys was used to give more specific results by rolling the mouse over the area of interest. A left mouse click allowed a tag to be placed on the part with the specific value for that location. Table 2 shows the

Figure 13. Ansys Cylindrical Support

Figure 14. Ansys Frictionless Support

Table 2. Comparison between Numerical Integration, Cosmos, and Ansys

Valve side @ 1000 lb		
Numerical Integration	Cosmos	Ansys
0.00466	0.004797	0.00466

Push rod side @ 1800 lb		
Numerical Integration	Cosmos	Ansys
------	0.001226	0.00105

Valve side @ 1333 lb		
Numerical Integration	Cosmos	Ansys
0.00621	0.005644	0.00621

Push rod side @ 2400 lb		
Numerical Integration	Cosmos	Ansys
------	0.001577	0.00139

comparison of a sampling of results from numerical integration, Cosmos, and Ansys. It is apparent that while Cosmos does not yield linear results for linear changes in force, both numerical integration and Ansys show linear results. Numerical integration and Ansys were used in the subsequent analysis of the baseline rocker arm and new designs.

2 RESULTS

2.1 Numerical Integration Results

Baseline Rocker Arm

Numerical integration was used to calculate stiffness (k) and mass moment of inertial (J) for the baseline rocker arm.

- The rotational inertia calculated from the numerical integration program was equal to $4.68 * 10^{-4}$ in-lb-sec^2. The stiffness was equal to 214592 lb/in.

Low Inertia Rocker Arm

Numerical integration was used to calculate stiffness (k) and mass moment of inertia (J) for a wide range of web thicknesses, widths, and delta heights. As previously stated, only one the valve side of the rocker arm was considered. The range of the parameters was the following:

Web thickness ranged from 0.1 to 0.5 in increments of 0.05 inches

Width ranged from 0.6 to 1.0 in increments of 0.1 inches

Delta height ranged from 0 to 0.6 in step of 0.1 inches.

- The goal of the design was to minimize rotational inertia, J, while maintaining stiffness, k. Therefore the quantity J/k should be minimized for the ideal design. The minimum was observed for width, web thickness, and delta height in figures 15 – 17, respectively. The minimum values width = 0.6, web thickness = 0.2, and 0.1 delta height succeeded in reducing the rotational inertia by 48%; however, the stiffness was reduced by 27%. These results violated the design specifications.

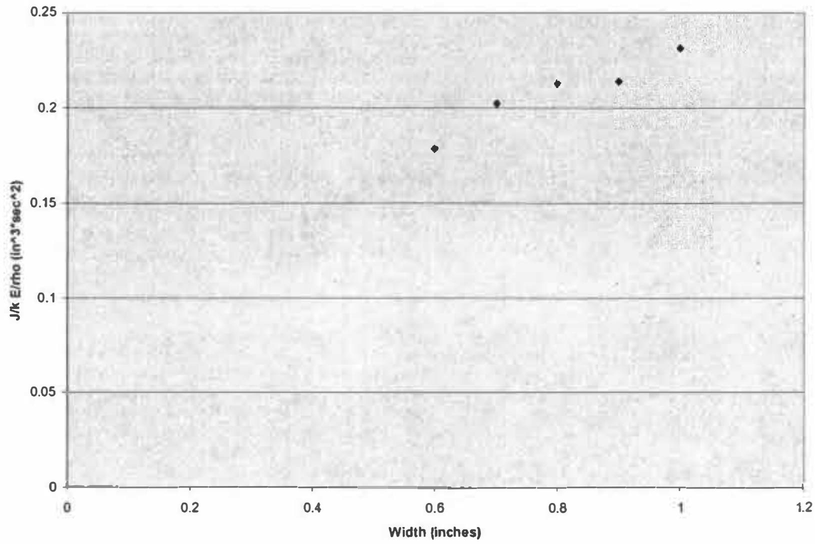

Figure 15. Width of Low Inertia Rocker Arm vs J/k Not Material Specific

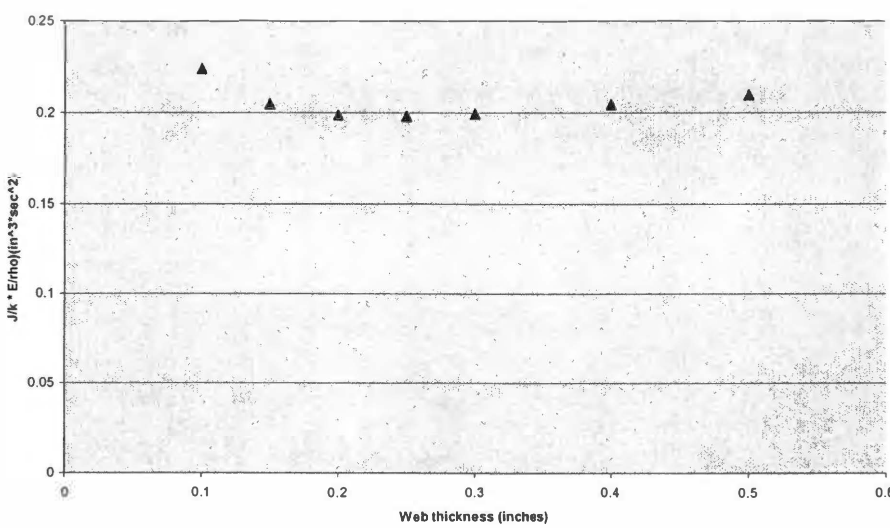

Figure 16. Web Thickness of Low Inertia Rocker Arm vs J/k Not Material Specific

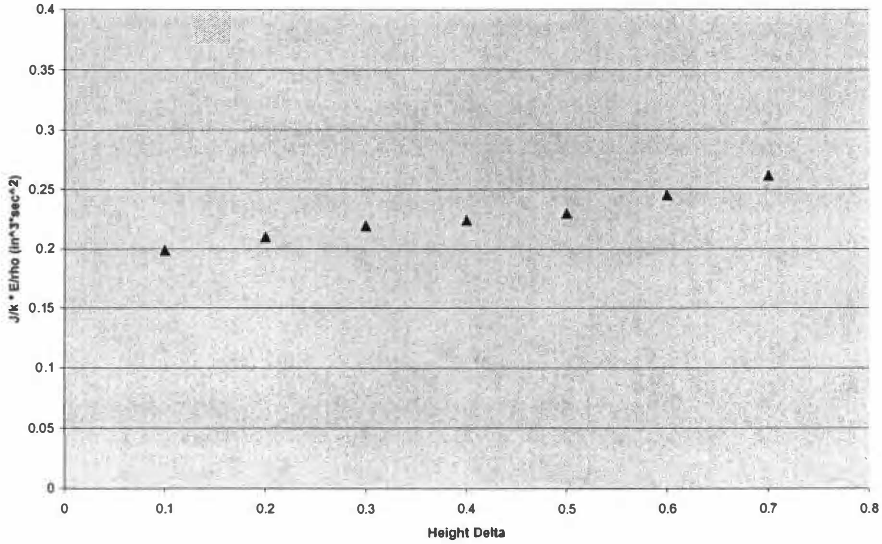

Figure 17. Delta Height of Low Inertia Rocker Arm vs J/k Not Material Specific

- The minimum values from the three J/k graphs did not produce the desired design. An iterative method was used to select the desired design. This iterative process was performed using the numerical integration program in figure A-3.
- The iterative process involved changing one of the quantities, width, web thickness, and delta height, while keeping the other two constant. The results were recorded and later compared.
- The results from the program yielded a width of 0.9 inch, web thickness of 0.1 inch, and delta height of 0.4 inch.
- The calculated rotational inertia was equal to $4.32*10^{-4}$ in-lb-sec^2.
- The calculated stiffness was equal to 212765 lb/in.

Increased Stiffness Rocker Arm

Numerical integration was used to calculate stiffness (k) and mass moment of inertia (J) for a wide range of web thicknesses, widths, and delta heights. As previously stated, only one the valve side of the rocker arm was considered. The range of the parameters was the following:

Web thickness ranged from 0.1 to 0.5 in increments of 0.05 inches

Width ranged from 0.6 to 1.0 in increments of 0.1 inches

Delta height ranged from 0 to 0.6 in step of 0.1 inches.

- The goal of the design was to maintain rotational inertia, J, while increasing stiffness, k. Therefore the quantity J/k should be minimized for the ideal design. The minimum was observed for width, web thickness, and delta height in figures 18 – 20, respectively. The minimum values width = 0.7 inch, web thickness =

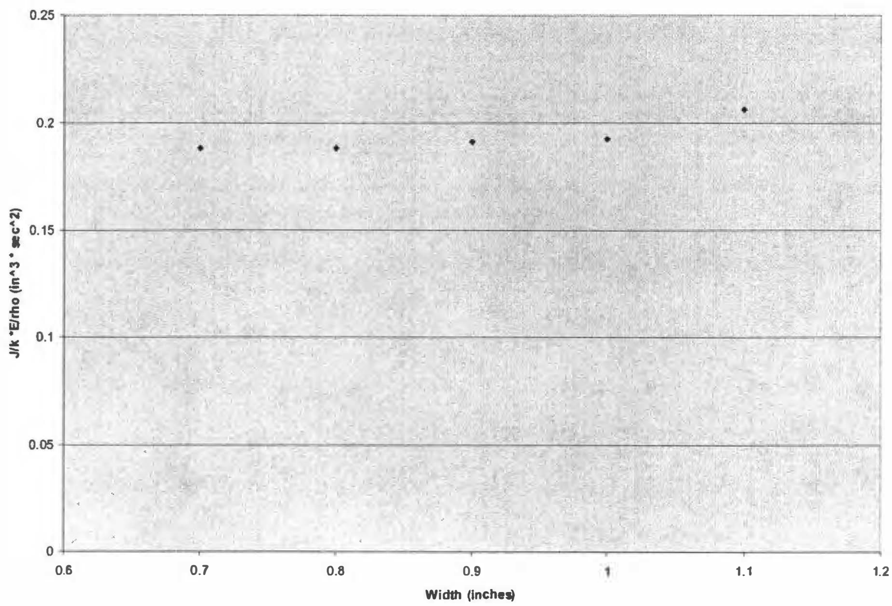

Figure 18. Width of Increased Stiffness Rocker Arm vs J/k Not Material Specific

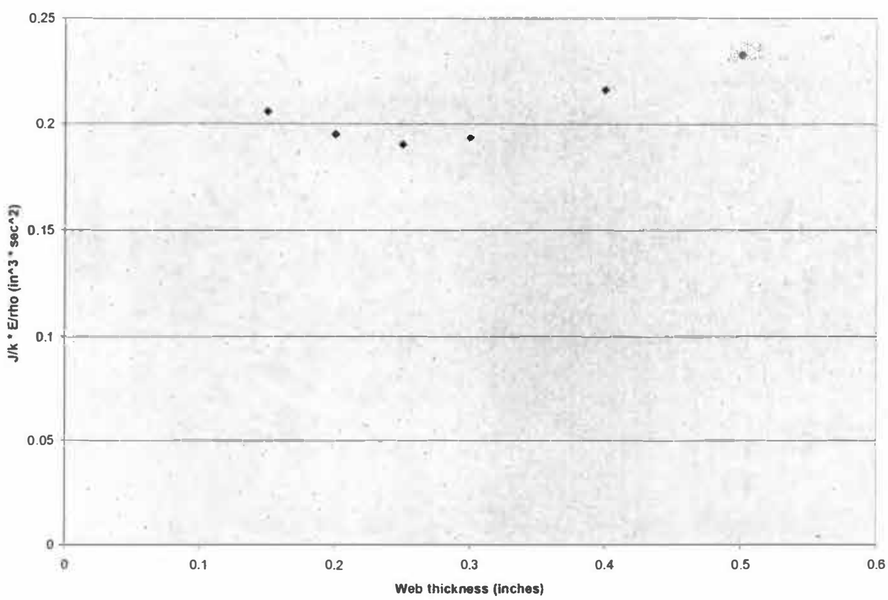

Figure 19. Web Thickness of Increased Stiffness vs J/k Not Material Specific

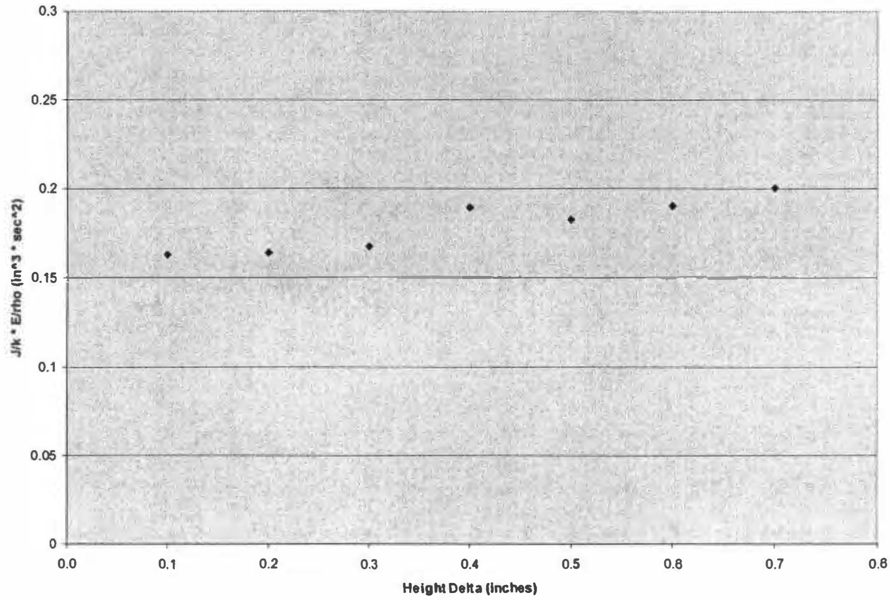

Figure 20. Delta Height of Increased Stiffness vs J/k Not Material Specific

0.25 inch, and 0.1 inch delta height succeeded in reducing the rotational inertia by 36%; however, the stiffness was reduced by 17%. These results violated the design specifications.

- The minimum values from the three J/k graphs did not produce the desired design. An iterative method was used to select the desired design. This iterative process was performed using the numerical integration program in figure A-3.
  The iterative process involved changing one of the quantities, width, web thickness, and delta height, while keeping the other two constant. The results were recorded and later compared.
- The results from the program yielded a width of 0.9 inch, web thickness of 0.25 inch, and delta height of 0.2 inch.
- The calculated rotational inertia was equal to $4.85*10^{-4}$ in-lb-sec^{2}. The calculated stiffness was equal to 238095 lb/in.

2.2 Inventor and Ansys Results

Baseline Rocker Arm

- The calculated rotational inertia from Inventor was $4.48*10^{-4}$ in-lb-sec^{2}.
- The deflection result from Ansys was 0.00466 inch and can be seen in figure 21.
- The stiffness was equal to 214592 lb/in.

Lower Inertia Rocker Arm

- The calculated rotational inertia from Inventor was $4.32*10^{-4}$ in-lb-sec^{2}.
- The deflection result from Ansys was 0.0047 inch and can be seen in figure 22.

Figure 21. Ansys Deflection of Baseline Rocker Arm

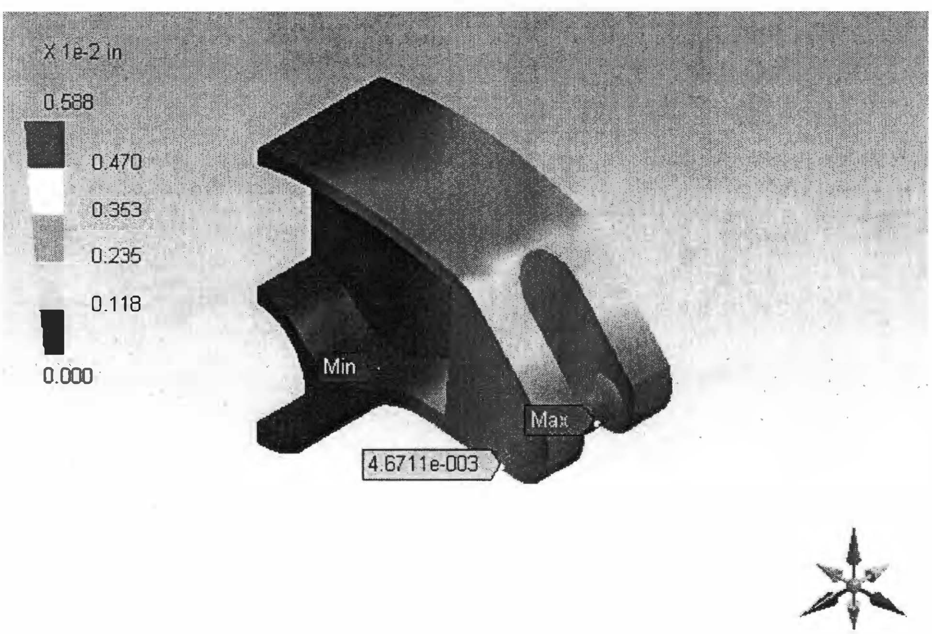

Figure 22. Ansys Deflection of Low Inertia Rocker Arm

- The stiffness was equal to 212765 lb/in.
- The improvement to the rotational inertia was 3%.
- Several scenarios were analyzed in Ansys to have a comparison to the numerical integration program. Figures 23 – 25 show the results. The numerical integration program was within 3% of the Ansys results.

Increased Stiffness Rocker Arm

- The calculated rotational inertia from Inventor was $4.66*10^{-4}$ in-lb-sec^2.
- The deflection result from Ansys was 0.0041" and can be seen in figure 26.
- The calculated stiffness was 243902 lb/in.
- The improvement to stiffness was 12%.

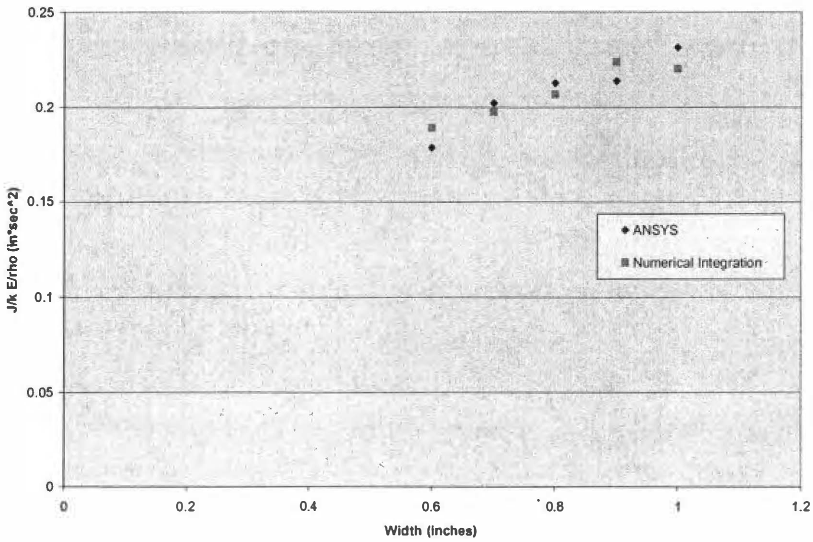

Figure 23. Ansys and Numerical Integration Width for Low Inertia vs J/k Not Material Specific

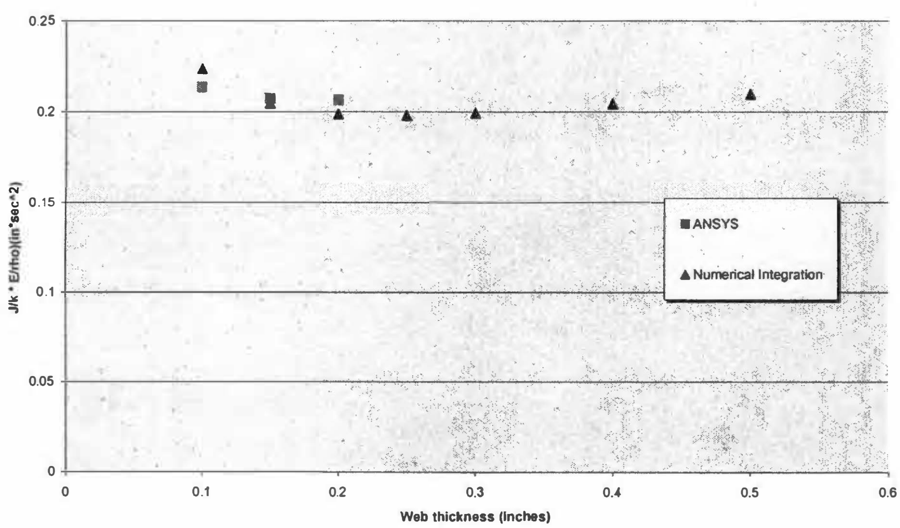

Figure 24. Ansys and Numerical Integration Web Thickness for Low Inertia vs J/k Not Material Specific

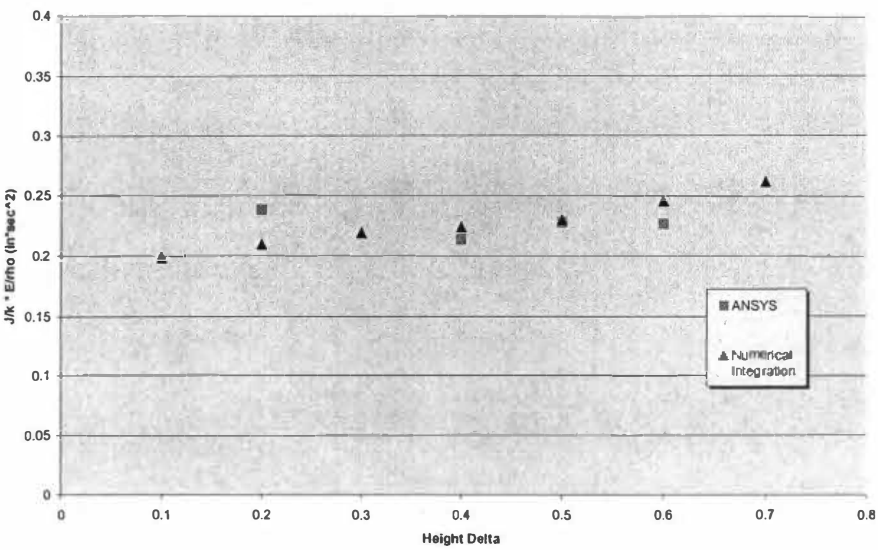

Figure 25. Ansys and Numerical Integration Delta Height for Low Inertia vs J/k Not Material Specific

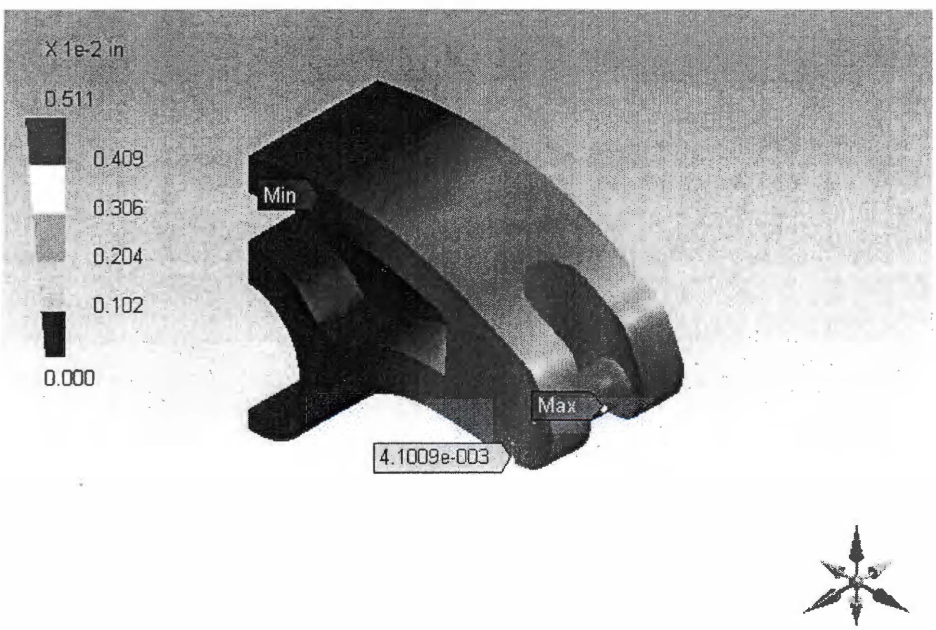

Figure 26. Ansys Deflection of Stiffer Rocker Arm

CONCLUSION

The goal was to improve the baseline rocker arm through two designs. One design was intended to exhibit lower rotational inertia while maintaining the baseline stiffness. The other design was intended to have higher stiffness while maintaining the baseline rotational inertia. It was expected that these improvements would be significant. While the results were not as profound as anticipated, some improvements were made. Table 3 shows a comparison of the results of the Jesel and the new designs. In the low inertia design, the rotational inertia was $4.32*10^{-4}$ in-lb-sec^2, which is a 3% improvement on the baseline rocker arm. In the stiffer design, the stiffness was 243,902 lb/in, which is a 12% improvement.

Table 3. Comparison of Results of Jesel Rocker Arm and New Designs

	Jesel	Low Inertia Design	High Stiffness Design
Rotational Inertia (in-lb-sec^2)	4.48*10^-4	4.32*10^-4	4.66*10^-4
Stiffness (lb/in)	214592	212765	243902

REFERENCES

1. Robert D. Cook and Warren C. Young, Advanced Mechanics of Materials (New Jersey : Prentice Hall 1999) 585.

2. G. R. Cowper, "The Shear Coefficient in Timoshenko's Beam Theory," Journal of Applied Mechanics (1966) : 335 – 339.

3. Russell C. Hibbeler, Mechanics of Materials (New Jersey : Prentice Hall 1994) 87.

4. R. C. Hibbeler, Engineering Mechanics Dynamics (New Jersey : Prentice Hall 1995) 343.

5. William T. Thomson and Marie Dillon Dahleh, Theory of Vibration with Applications (New Jersey : Prentice Hall 1998) 16.

APPENDIX

I-Beam vs H-Beam Program

$l := 2$ Length

$b := .9$ Width

$q := .1$ Web Thickness

$bot(x) := -.5 \quad top(x) := 1$

$h(x) := top(x) - bot(x)$ Height

$F := 1000$ Force

$E := 10 \cdot 10^6$ modulus of elasticity

$\rho := 0.098$

$initial := \begin{bmatrix} 0 \\ 0 \end{bmatrix}$ initial conditions at fixed end of y(0) = 0 & dy(0) = 0

I – Beam

$$ycg(x) := \frac{(top(x) + bot(x))}{2}$$

$$aa(x) := b \cdot h(x) - ((b - q) \cdot (h(x) - 2 \cdot q))$$

$$r(x) := x^2 + ycg(x)^2$$

$$I(x) := \frac{b \cdot (h(x))^3}{12} - \frac{1}{12} \cdot (b - q) \cdot (h(x) - 2 \cdot q)^3$$

$$P(x) := (r(x) \cdot aa(x) + I(x)) \cdot \rho$$

$$D(x,y) := \begin{bmatrix} y_1 \\ \frac{F \cdot (x - 1)}{E \cdot I(x)} \end{bmatrix}$$

$$J_1 := \int_0^2 P(x)\,dx$$

$$Z := rkfixed(initial, 0, 2, 500, D)$$

H – Beam

$$ycg(x) := \frac{(top(x) + bot(x))}{2}$$

$$aaa(x) := b \cdot h(x) - ((b - 2 \cdot q) \cdot (h(x) - q))$$

$$r(x) := x^2 + ycg(x)^2$$

$$I_1(x) := \frac{b \cdot (h(x))^3}{12} - \frac{1}{12} \cdot (b - 2 \cdot q) \cdot (h(x) - q)^3$$

$$P(x) := (r(x) \cdot aaa(x) + I_1(x)) \cdot \rho$$

$$D_1(x,y) := \begin{bmatrix} y_1 \\ \frac{F \cdot (x - 1)}{E \cdot I_1(x)} \end{bmatrix}$$

$$J_2 := \int_0^2 P(x)\,dx$$

$$Z_1 := rkfixed(initial, 0, 2, 500, D_1)$$

$J_1 =$ $\quad (Z^{<1>})_{500} =$ $\quad$ I – beam

$J_2 =$ $\quad (Z_1^{<1>})_{500} =$ $\quad$ H – beam

Figure A- 1. Sample Calculations of I-beam vs. H-beam

Baseline Rocker Arm Program

$l := 2.127$ Length

$b := .9$ Width

$F := 1000$ Force

$sf := 1.2$

$E := 10 \cdot 10^6$ modulus of elasticity

$\rho := 0.098$

$G := \dfrac{E}{(2 \cdot 1.33)}$

$initial := \begin{bmatrix} 0 \\ 0 \end{bmatrix}$ initial conditions at fixed end of y(0) = 0 & dy(0) = 0

$$top(x) := -.0852 \cdot x^6 + .4923 \cdot x^5 - 1.0305x^4 + .9425 \cdot x^3 - .5602 \cdot x^2 + .3451 \cdot x + .9454$$

$$bot(x) := -1.2981 \cdot x^6 + 7.1569x^5 - 13.844x^4 + 10.175x^3 - 1.2301 \cdot x^2 - 0.0674x - .6289$$

$h(x) := top(x) - bot(x)$ Height

Middle Section

$$ycg(x) := \frac{(top(x) + bot(x))}{2}$$

$$aa(x) := b \cdot h(x)$$

$$r(x) := x^2 + ycg(x)^2$$

$$I(x) := \frac{b \cdot (h(x))^3}{12}$$

$$P(x) := (r(x) \cdot aa(x) + I(x)) \cdot \rho$$

$$D(x, y) := \begin{bmatrix} y_1 \\ \dfrac{F \cdot (x - 1.9)}{E \cdot I(x)} \end{bmatrix}$$

$$J_1 := \int_{.375}^{1.5} P(x)\,dx$$

$$Z := rkfixed(initial, .375, 1.5, 500, D)$$

$$Z_{sh} := \int_{.375}^{1.5} \frac{F \cdot sf}{aa(x) \cdot G}\,dx$$

Figure A- 2. Numerical Integration Program for Baseline Rocker Arm

End Calculations

$$I_1\cancel{(x)} := \frac{h(x)^3 \cdot b}{12} - \frac{h(x)^3 \cdot .37}{12}$$

$$aaa(x) := (h(x) \cdot b) - (h(x) \cdot .37)$$

$$P_1(x) := \left(r(x) \cdot aaa(x) + I_1(x)\right) \cdot \rho$$

$$D_1(x, y) := \begin{bmatrix} y_1 \\ \dfrac{F \cdot (x - 1.9)}{E \cdot I_1(x)} \end{bmatrix}$$

$$Z_1 := \text{rkfixed}\left(\text{initial}, 1.5, 1.9, 500, D_1\right)$$

$$J_2 := \int_{1.5}^{2.127} P_1(x)\,dx$$

$$Z_{sh1} := \int_{1.5}^{1.9} \frac{F \cdot sf}{aaa(x) \cdot G}\,dx$$

Hole Cut

$$yc1(x) := \sqrt{.375^2 - x^2}$$

$$yc2(x) := -yc1(x)$$

$$ht(x) := top(x) - yc1(x)$$

$$hb(x) := -bot(x) - yc1(x)$$

$$aba(x) := b \cdot ht(x)$$

$$ab(x) := -b \cdot (bot(x) - yc2(x))$$

$$ycg1(x) := \frac{\left[ab(x) \cdot \left(yc1(x) + \frac{hb(x)}{2}\right)\right] + aba(x) \cdot \left(yc1(x) + \frac{ht(x)}{2}\right)}{ab(x) + aba(x)}$$

$$y11(x) := \left(yc1(x) + \frac{top(x) - yc1(x)}{2}\right) - ycg1(x)$$

Figure A-2. Continued

$$y22(x) := \left(yc2(x) + \frac{bot(x) - yc2(x)}{2}\right) - ycg1(x)$$

$$r2(x) := x^2 + ycg1(x)^2$$

$$Ij(x) := \frac{b \cdot ht(x)^3}{12} + \left(aba(x) \cdot y11(x)^2\right) + \frac{b \cdot hb(x)^3}{12} + ab(x) \cdot y22(x)^2$$

$$abc(x) := aba(x) + ab(x)$$

$$P_3(x) := (r2(x) \cdot abc(x) + Ij(x)) \cdot \rho$$

$$D_3(x, y) := \begin{bmatrix} y_1 \\ \dfrac{F \cdot (x - 1.9)}{E \cdot Ij(x)} \end{bmatrix}$$

$$Z_3 := \mathrm{rkfixed}(\mathrm{initial}, 0, .375, 500, D_3)$$

$$J_3 := \int_0^{.375} P_3(x)\,dx$$

$$Z_{sh3} := \int_0^{.375} \frac{F \cdot sf}{abc(x) \cdot G}\,dx$$

$$y := \left(Z_1^{\langle 2 \rangle}\right)_{500} + \left(Z_3^{\langle 2 \rangle}\right)_{500} + \left(Z^{\langle 2 \rangle}\right)_{500}$$

$$y_s := -Z_{sh} + -Z_{sh1} + -Z_{sh3}$$

$$y_t := y + y_s$$

$$J_r := J_1 + J_2 + J_3$$

Figure A-2. Continued

IBeam Rocker Arm Program

$l := 2.127$ Length

$F := 1000$ Force

$sf := 2.5$

$b := .9$ Width

$E := 10 \cdot 10^6$ modulus of elasticity

$q := .1$ Web Thickness

$\rho := 0.098$

$G := \dfrac{E}{(2 \cdot 1.33)}$

$initial := \begin{bmatrix} 0 \\ 0 \end{bmatrix}$ initial conditions at fixed end of y(0) = 0 & dy(0) = 0

$top(x) := .0456x^6 - .2326x^5 + .4197 \cdot x^4 - .4229 \cdot x^3 + .0586x^2 + .2295x + 1.3507 + .3$

$bot(x) := .0302 \cdot x^6 - .3264x^5 + 1.5867x^4 - 3.4759x^3 + 2.9738x^2 - .0287 \cdot x - .4783$

$h(x) := top(x) - bot(x)$ Height

Middle Section

$ycg(x) := \dfrac{(top(x) + bot(x))}{2}$

$aa(x) := b \cdot h(x) - ((b - q) \cdot (h(x) - 2 \cdot q))$

$r(x) := x^2 + ycg(x)^2$

$I(x) := \dfrac{b \cdot (h(x))^3}{12} - \dfrac{1}{6} \cdot \left(\dfrac{b}{2} - \dfrac{q}{2}\right) \cdot (h(x) - 2 \cdot q)^3$

$P(x) := (r(x) \cdot aa(x) + I(x)) \cdot \rho$

$D(x, y) := \begin{bmatrix} y_1 \\ \dfrac{F \cdot (x - 1.9)}{E \cdot I(x)} \end{bmatrix}$

$J_1 := \displaystyle\int_{.375}^{1.375} P(x)\,dx$

$Z := rkfixed(initial, .375, 1.375, 500, D)$

$Z_{sh} := \displaystyle\int_{.375}^{1.375} \dfrac{F \cdot sf}{aa(x) \cdot G}\,dx$

Figure A- 3. Numerical Integration Program of I-beam Rocker Arm

End Calculations

$$I_1(x) := \frac{h(x)^3 \cdot b}{12} - \frac{h(x)^3 \cdot .37}{12}$$

$$aaa(x) := (h(x) \cdot b) - (h(x) \cdot .37)$$

$$P_1(x) := \left(r(x) \cdot aaa(x) + I_1(x)\right) \cdot \rho$$

$$D_1(x, y) := \begin{bmatrix} y_1 \\ \dfrac{F \cdot (x - 1.9)}{E \cdot I_1(x)} \end{bmatrix}$$

$$Z_1 := \mathrm{rkfixed}\left(\mathrm{initial}, 1.5, 1.9, 500, D_1\right)$$

$$J_2 := \int_{1.5}^{2.127} P_1(x)\, dx$$

$$Z_{sh1} := \int_{1.5}^{1.9} \frac{F \cdot sf}{aaa(x) \cdot G}\, dx$$

Solid Transition

$$I_2(x) := \frac{h(x)^3 - b}{12}$$

$$aaaa(x) := h(x) \cdot b$$

$$P_2(x) := \left(r(x) \cdot aaaa(x) + I_2(x)\right) \cdot \rho$$

$$D_2(x, y) := \begin{bmatrix} y_1 \\ \dfrac{F \cdot (x - 1.9)}{E \cdot I_2(x)} \end{bmatrix}$$

$$Z_2 := \mathrm{rkfixed}\left(\mathrm{initial}, 1.375, 1.5, 500, D_2\right)$$

$$J_3 := \int_{1.375}^{1.5} P_2(x)\, dx$$

$$Z_{sh2} := \int_{1.5}^{1.9} \frac{F \cdot sf}{aaaa(x) \cdot G}\, dx$$

Figure A-3. Continued

Hole Cut

$$yc1(x) := \sqrt{.375^2 - x^2}$$

$$yc2(x) := -yc1(x) + .125$$

$$ht(x) := top(x) - yc1(x)$$

$$hb(x) := -yc2(x)$$

$$aba(x) := b \cdot ht(x) - (ht(x) - 2 \cdot q) \cdot (b - q)$$

$$ab(x) := b \cdot (yc2(x) - bot(x))$$

$$ycg1(x) := \frac{\left[ab(x) \cdot \left(yc2(x) + \frac{hb(x)}{2}\right)\right] + aba(x) \cdot \left(yc1(x) + \frac{ht(x)}{2}\right)}{ab(x) + aba(x)}$$

$$y11(x) := \left(yc1(x) + \frac{top(x) - yc1(x)}{2}\right) - ycg1(x)$$

$$y22(x) := \left(yc2(x) + \frac{bot(x) - yc2(x)}{2}\right) - ycg1(x)$$

$$r2(x) := x^2 + ycg1(x)^2$$

$$Ij(x) := \frac{b \cdot ht(x)^3}{12} - \frac{(b - q) \cdot (ht(x) - 2 \cdot q)^3}{12} + \left(aba(x) \cdot y11(x)^2\right) + \frac{b \cdot hb(x)^3}{12} + ab(x) \cdot y22(x)^2$$

$$abc(x) := aba(x) + ab(x)$$

$$P_3(x) := (r2(x) \cdot abc(x) + Ij(x)) \cdot \rho$$

$$D_3(x, y) := \begin{bmatrix} y_1 \\ \frac{F \cdot (x - 1.9)}{E \cdot Ij(x)} \end{bmatrix}$$

$$Z_3 := \text{rkfixed}\left(\text{initial}, 0, .375, 500, D_3\right)$$

$$J_4 := \int_0^{.375} P_3(x)\,dx$$

$$Z_{sh3} := \int_0^{.375} \frac{F \cdot sf}{abc(x) \cdot G}\,dx$$

Figure A-3. Continued

$$y := \left(Z_1^{<2>}\right)_{500} + \left(Z_2^{<2>}\right)_{500} + \left(Z_3^{<2>}\right)_{500} + \left(Z^{<2>}\right)_{500}$$

$$y_s := -Z_{sh} + -Z_{sh1} + -Z_{sh2} + -Z_{sh3}$$

$$J := J_1 + J_2 + J_3 + J_4$$

Figure A-3. Continued

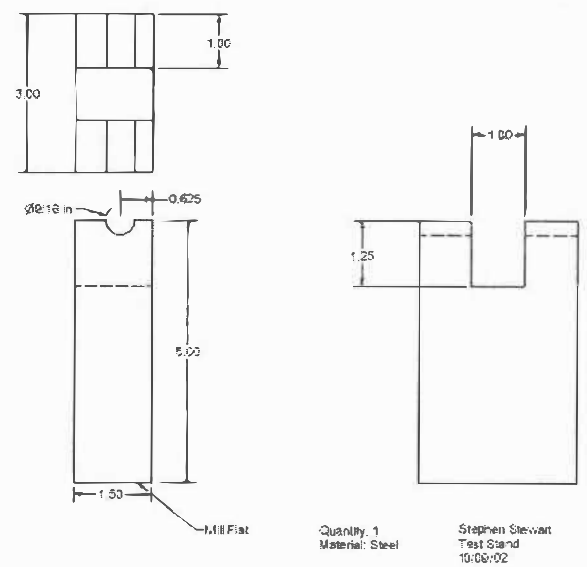

Figure A- 4. Detail Drawing of Test Stand

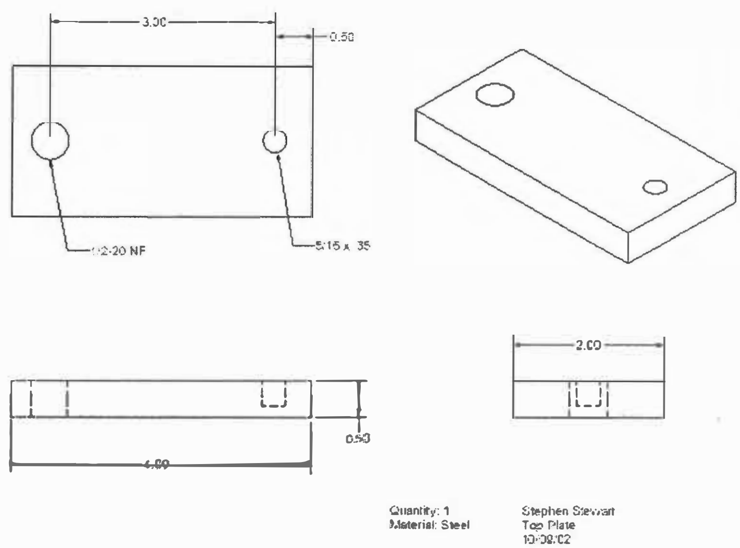

Figure A- 5. Detail Drawing of Top Plate

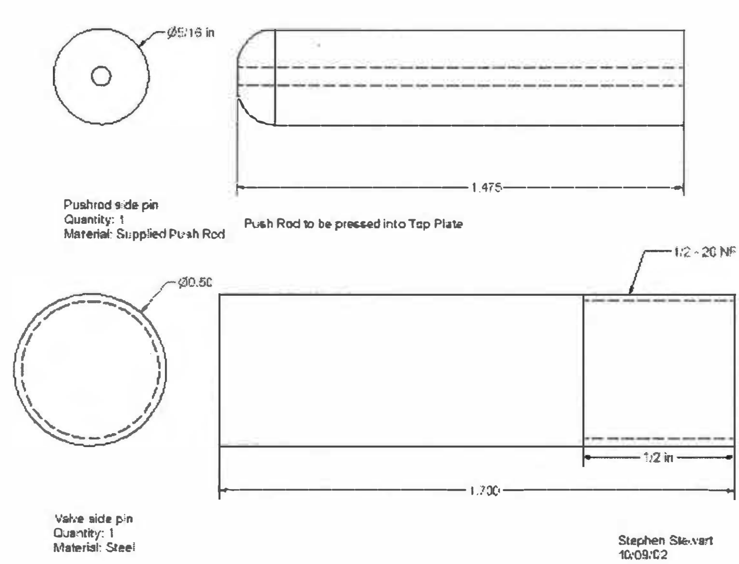

Figure A- 6. Detail Drawing of Pushrod and Valve Side Pin

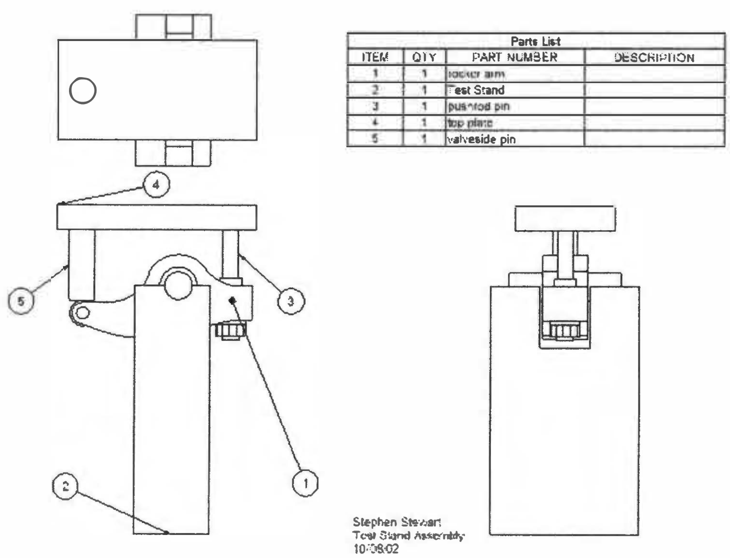

Figure A- 7. Assembly Drawing of Test Stand

VITA

Stephen Edward Stewart was born on January 29, 1977 in Nashville, TN. He attended Nashville public schools until his graduation from McGavock High School in May of 1995. The following August, he began his undergraduate studies at the University of Tennessee, Knoxville. After earning a Bachelor of Science in Mechanical Engineering in December 1999, he was employed by Newport News Shipbuilding in Newport News, VA. In 2001, he returned to the University of Tennessee to pursue a Master of Science in Mechanical Engineering.